

Numerical analysis for predicting the operability window of slot-die coating onto porous media

Tomomi Goda^{1, a)}, Yuichi Sasaki^{1, b)}, Mamoru Mizuno^{2, c)}, Kazuhiko Morizawa^{1, d)},
Hitoshi Katakura^{1, e)} and Shigetaka Tomiya^{1, f)}

1) Advanced Materials Laboratories, Sony Corporation.

Atsugi Tec. 4-14-1 Asahi-cho, Atsugi-shi, Kanagawa, 243-0014 Japan

2) Sony Energy Device Corporation.

1-1 Shimosugishita, Hiwadamachitakakura, Koriyama-shi, Fukushima, 963-0531 Japan

Introduction

In a wide range of industries, such as paper, electronics, energy, and medicine, processed film is used to serve various functions. Coating onto porous media is critically important for forming composite functional thin films. A major technical concern for accurate prediction of this process is that one has to deal with the flow of coating bead and the penetration process. Because the pressure in a coating bead is difficult to determine, most previous studies have treated the flows in the porous media and the coating bead separately using simplified models. Recently, analytical models simultaneously dealing with both phenomena have been proposed [1, 2]; however, Xiaoyu Ding et al.'s [1] study of penetration depth is limited in its applicability to a defect-free coating condition. The operability window for slot-die coating of porous media has been discussed, but no experimental data concerning coating boundary conditions could be found [2]. Furthermore, the substrate-support system is important for accurate prediction. Previous models have assumed that coating is done on flat porous substrates. In slot-die coating systems based on a roll-to-roll process, the curvature of the back-up roll needs to be considered for the "on-roll" coating method.

Here, we investigate slot-die coating of porous media with the aim of estimating not only the penetration depth but also the practical operability window using two-dimensional numerical analysis. For this purpose, both bead pressure and capillary pressure are considered as driving forces of the penetration. Moreover, the curvature of the slot-die backup-roll is also taken into account for precise estimation. We also present an experimental result for the air-entrainment boundary in the operability window of a defect-free film.

Experimental setup

A schematic of the coating equipment is shown in Fig.1 (a). A slot die opposite a back-up roll is placed at an angle of $\theta_R = 20^\circ$ from the vertical. Liquid is coated onto a porous medium, which is formed on a solid film. Porous media in this study have high hydrophilic nature. A schematic of the slot die is shown in Fig.1 (b). It has a slot gap of $W = 150 \mu\text{m}$, an upstream die-lip length of $L_u = 1.5 \text{ mm}$, a downstream die-lip length of $L_d = 1.9 \text{ mm}$, and a back-up roll radius of $R = 70 \text{ mm}$. x is the coating-bead length (or the position of the upstream meniscus) and h is the penetration depth. These

a) E-mail: Tomomi.Goda@sony.com, Tel: +81-50-3140-8796, Fax: +81-50-3809-2000

b) E-mail: Yuichi.Sasaki@sony.com

c) E-mail: Mamoru.Mizuno@sony.com, Present address: Advanced Materials Laboratories, Sony Corporation

d) E-mail: Kazuhiko.Morizawa@sony.com

e) E-mail: Hitoshi.Katakura@sony.com

f) E-mail: Shigetaka.Tomiya@sony.com

two parameters are estimated by numerical analysis. Other processing parameters and material properties are listed in Table 1. The coating thickness is set to a constant value. Therefore, the feed-flow rates vary as functions of coating speed. Capillary pressure, one of the driving forces behind penetration, is calculated by the Young–Laplace equation to be 250 kPa.

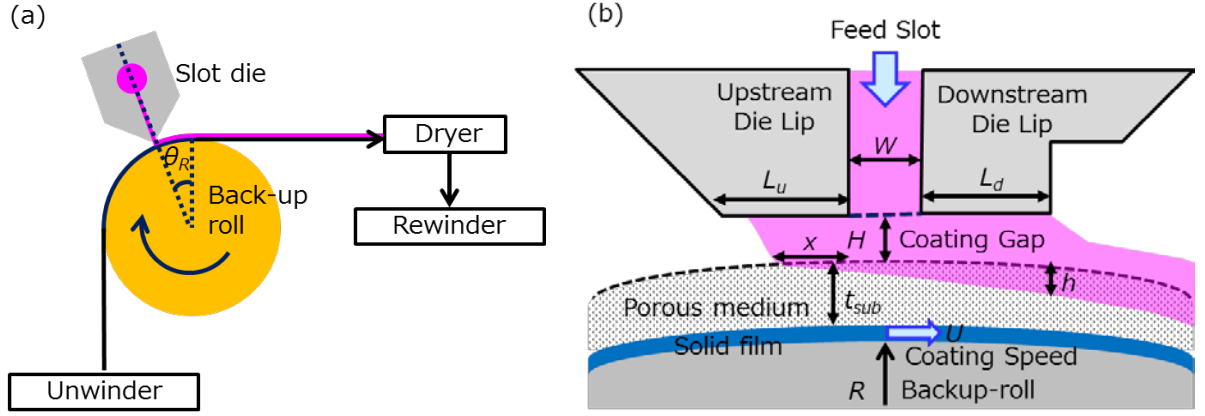


Fig.1 (a) Scheme of the experimental setup; (b) scheme of slot-die coating onto porous media

Table 1: Processing parameters and material properties for the coating experiment

| Parameter | Unit | Value |
|---------------------------------------|-------------------------|-----------------------|
| Coating thickness (no penetration) | T μm | 31 |
| Porous media thickness | t_{sub} μm | 42 |
| Coating gap | H μm | 16–61 |
| Coating speed | U m/min | 5 and 20 |
| Liquid density | ρ kg/m^3 | 1250 |
| Liquid viscosity | μ Pa·s | 0.021 |
| Porosity | ε — | 0.152 |
| Surface tension | γ mN/m | 28.9 |
| Contact angle | θ $^\circ$ | 17.1 |
| Mode pore diameter | D μm | 0.44 |
| Permeability | K m^2 | 4.0×10^{-16} |

Numerical model

In this study, we implemented two-dimensional (2D) numerical analysis using the commercial computational fluid dynamics (CFD) simulation software FLOW-3D (Flow Science Inc.) [3], which calculates free surface flow using the finite difference method (FDM). Coating-bead flow and penetration flow are based on the Navier–Stokes equation and Darcy’s law [4], respectively.

Previous studies have been used one dimensional (1D) depth dependence Darcy’s law for

penetration-flow calculation into porous media [1, 2]. Porous media dealt with in this study is highly hydrophilic. In addition, capillary pressure into porous media is thought to be larger than bead pressure at surface of porous media. In this case, it should be taken into account of not only 1D depth dependence but also other directions. Thus, we adopted 2D numerical analysis.

The operability windows of two kinds of the coating defects, dripping and air entrainment, are estimated from the coating-bead length, x . In various previous studies of coating on a solid substrate, the position of an upstream meniscus was used as an indicator of the coating-limit boundary [5-7]. When x becomes a negative value, air entrainment can occur, while x becomes larger than L_u , dripping can occur. Here, it is noted that we assume that coating on a porous medium approximates coating on a solid substrate since experimental data for measuring coating bead on porous media could be hard to be acquired.

Results and discussion

The operability-window results for coating on porous and non-porous media are shown in Fig.2 and Table 2. These results constitute maps for optimizing the coating gap under constant coating thickness. The operability window was estimated from coating-bead length, which was calculated in Fig.2 (a). Dripping could occur in the upper gray zone and air entrainment could occur in the lower gray zone. It was also clearly seen that the operability window on porous media shifted toward lower coating gaps than that on non-porous media. Fig.2 (b) shows the relationship between coating speeds and coating gaps obtained from Fig.2 (a). It can be observed that the operability window depended on coating speed only for coating on a porous medium in this study. The operability window for the 5-m/min case shifted farther than that for the 20-m/min case. These CFD results were then compared with the experimental results for the air-entrainment boundary. Table 2 presents the experimental conditions and coating gap results in the defect-free and air-entrainment cases. These results closely match the predictions; we can see the same tendency regarding the difference between the CFD and experimental results of non-porous and porous media under both coating speeds. The air-entrainment boundary for the operability window was well estimated and consistent with the experiment results.

Therefore, it is conceivable that the operability window shifted in accordance with liquid penetration in porous media. Accordingly, the penetration depth under both coating speeds for the above CFD data is compared in Fig.3. The vertical axis is the penetration depth. In upper region of Fig.3, the penetration depth is more, whereas it is less in the lower region. It can be seen that the penetration depth for 5 m/min was deeper than that for 20 m/min. Moreover, the penetration depth slightly increases as the coating gap reduces. We note here that it is observed that penetration depth for 5m/min became saturated as the coating gap got narrower. This is because penetration depth in this case reached the value of porous media thickness which we initially set in this study.

The total flow rate is equal to the sum of the coating-bead flow rate and the penetration flow rate. The penetration in the porous media reduced the coating-bead flow rates, and thus the coating-bead

pressure declined. Therefore, the operability window on porous media shifted toward lower coating gaps than that on non-porous media.

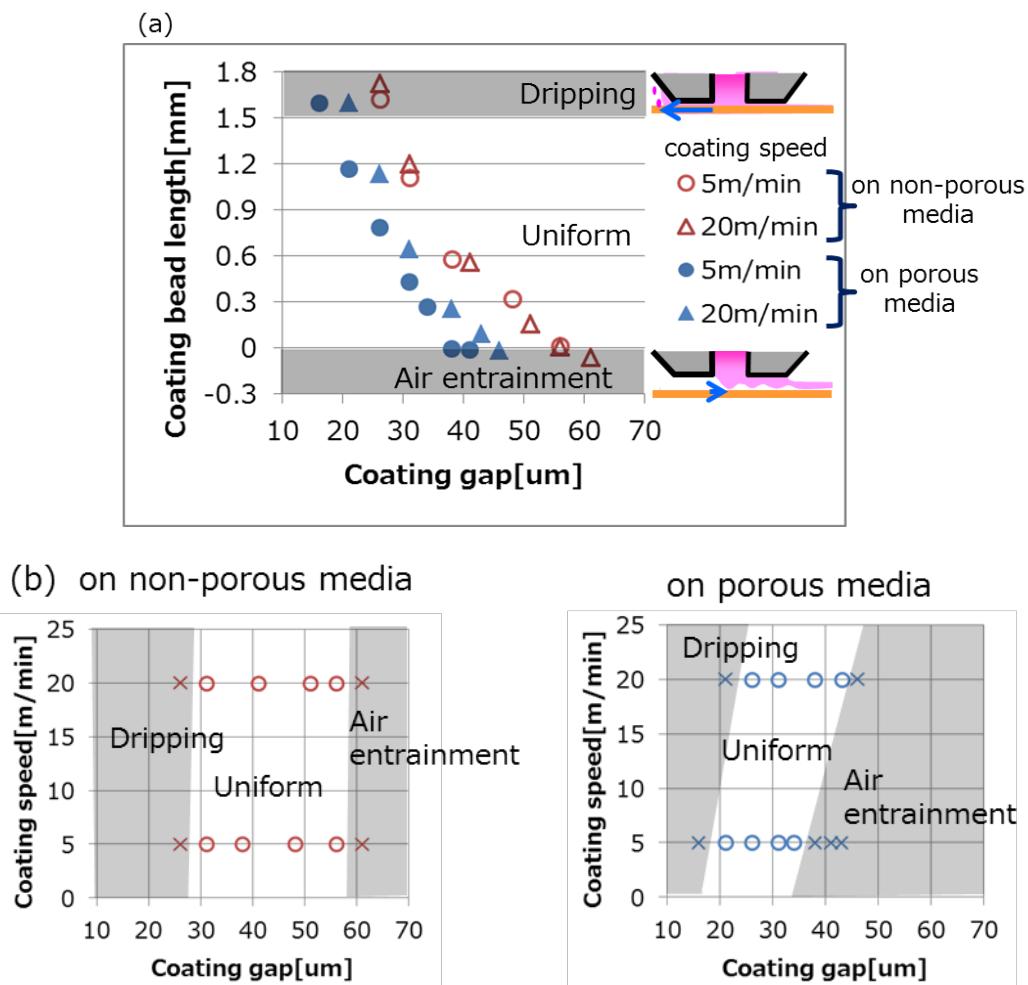


Fig.2 Effect of penetration and coating speed upon the operability window, (a) coating gap vs. coating-bead length, (b) coating gap vs. coating speed. Defect-free cases are plotted by “O” and coating-defect cases are plotted by “X” in (b).

Table 2: Experimental results

| Experiment No. | Substrate | Coating speed | Coating gap | Film quality |
|----------------|------------|---------------|-------------|-----------------|
| 1 | Non-porous | 20 m/min | 56 μm | Defect free |
| 2 | | | 61 μm | Air entrainment |
| 3 | Porous | 20 m/min | 43 μm | Defect free |
| 4 | | | 48 μm | Air entrainment |
| 5 | | 5 m/min | 34 μm | Defect free |
| 6 | | | 38 μm | Air entrainment |

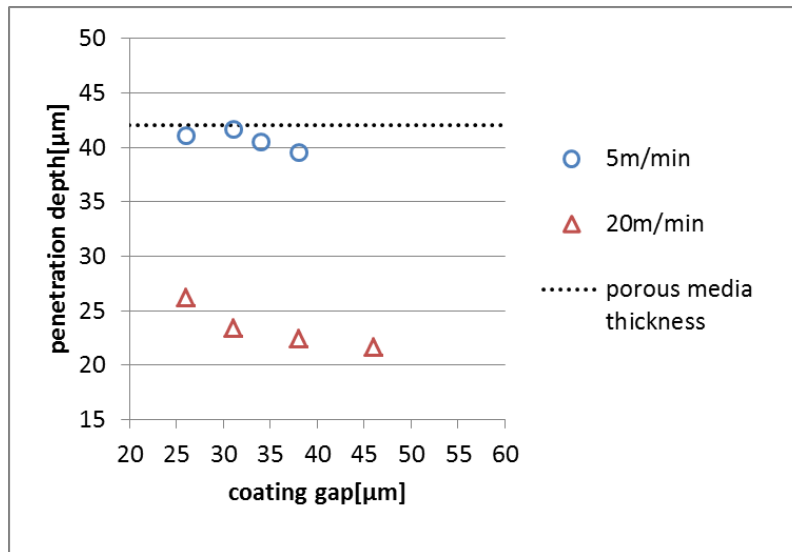


Fig.3 Effect of coating speed upon penetration depth. When coating speed was 5 m/min, the penetration depth reached the bottom of the porous medium.

Conclusions

We performed numerical analysis and experiments to investigate the operability window and penetration depth for slot-die coating onto porous media. Using a numerical model based on the actual coating equipment, substrate, and conditions, the operability window was well estimated. This model will be applied to investigate the effects of various material parameters.

Reference

- [1] X. Ding, J.P. Ebin, T.A.L. Harris, Z. Li, T.F. Fuller, *AIChE*, p.4231 vol.60, 2014
- [2] X. Ding, Doctor Thesis, Georgia Institute of Technology, 2014
- [3] Flow Science, Inc., *FLOW-3D Documentation*, Release 11.0.0, 2014
- [4] S. Whitaker, *Transport in Porous Media*, p.3 vol.1, 1986
- [5] C. Lin, D.S.H. Wong, T. Liu, P. Wu, *Advances in Polymer Technology*, p.31 vol.29, 2010
- [6] S.H. Lee, H.J. Koh, B.K. Ryu, S.J. Kim, H.W. Jung, J.C. Hyun, *Chemical Engineering Science*, p.4953 vol.66, 2011
- [7] H.S. Ji, W. Ahn, I. Kwon, J. Nam, H.W. Jung, *Chemical Engineering Science*, p.122 vol.143, 2016